

Determining Hadron-Quark Phase Transition Chemical Potential via Astronomical Observations

Zhan Bai^{1,2,*} and Yu-xin Liu^{1,2,3,†}

¹*Department of Physics and State Key Laboratory of Nuclear Physics and Technology, Peking University, Beijing 100871, China*

²*Collaborative Innovation Center of Quantum Matter, Beijing 100871, China*

³*Center for High Energy Physics, Peking University, Beijing 100871, China*

(Dated: April 1, 2019)

We propose a scheme to determine the chemical potential and baryon number density of the hadron-quark phase transition in cold dense strong interaction matter (compact star matter). The hadron matter is described with the relativistic mean field theory, and the quark matter is described with the Dyson-Schwinger equation approach of QCD. To study the first-order phase transition, we take the sound speed as the interpolation objective to construct the equation of state in the middle density region. With the maximum mass, the tidal deformability and the radius of neutron stars being taken as calibration quantities, the phase transition chemical potential is constrained to a quite small range. And the most probable value of the phase transition chemical potential is found.

Introduction: Researches on the phase transitions of strong interaction matter (simply, QCD phase transition) have attracted great attentions in recent years. On theoretical side, the lattice QCD, the Dyson-Schwinger (DS) equation approach, the functional renormalization group (FRG) approach and many effective models have made great progress in the studies (see, e.g., Refs. [1–6]). However, even with the chiral susceptibility criterion identifying the phase transition (e.g., Ref. [3]), the chemical potential region for the hadron–quark phase transition to occur has not yet been settled down well. Besides, none of these approaches has provided a unified lagrangian which can describe naturally both the hadron matter at low density and the quark matter at high density simultaneously.

Because of the lack of a fundamental approach at present stage, to take into account the hadron-quark phase transition in the theoretical investigations, one usually take the way that describes the hadron matter and the quark matter separately via respective approach, and combine them together to get the complete equation of state (EoS) in the whole density region with constructions, for instance the Gibbs construction (see, e.g., Refs. [7]), the 3-window construction (for recent review, see, e.g., Ref. [8]), and so forth. In the Gibbs construction, even though the chemical potential region for the hadron-quark phase transition to occur can be fixed with the quark fraction $\chi = 0, 1$, respectively, one usually doubts the reliability of the result since it results from the assumption that the hadron model and the quark model are accurate at all densities. In fact, although the hadron model is accurate at saturation density because it has been calibrated with plenty of experimental data, different models give results deviating from each other greatly in the phase transition region [9, 10]. This means that the hadron model becomes unreliable in the phase transition region. Similar problem exists for the quark models. In the 3-window construction model, even though the above mentioned problems can be avoided, the chemical poten-

tials at which the phase transition occurs are assigned artificially.

It is well known that a first-order phase transition involves a phase coexistence region, and the EoS is not smooth at the states where the phase coexistence region begins, disappears, respectively. Consequently, the speed of sound, which is the derivative of the EoS, is discontinuous at the boundaries. Therefore, if we make use of the speed of sound to do the interpolation, we can study the phase transition with 3-window construction.

On experimental side, one can generate the matter at high temperature and low density even the warm dense matter with relativistic heavy ion collisions (RHICs) in laboratory and study the phase transitions. However, one can not get the very cold dense matter on earth. Therefore, one must take aid of astronomical observations, especially those for neutron stars [7, 8, 10–12], since neutron star is one of the most compact objects in the universe and it is believed that there exists hadron-quark phase transition in its central region.

One important property of neutron stars that can be observed on earth is their mass. Several years ago, two neutron stars with large mass (around $2M_{\odot}$) were observed [13, 14], which indicates that the EoS of the composing matter is stiff. Another important observation of neutron star is the gravitational wave. The detection of gravitational wave GW170817 in binary neutron star merger [15, 16] manifests that the tidal deformability of a $1.4M_{\odot}$ neutron star ($\Lambda_{1.4}$) is most probably smaller than 800 [16]. This means that the EoS is soft. Therefore, considering simultaneously the mass, the tidal deformability and other observables can provide strong constraints on the EoS of neutron star matter, and in turn, the hadron-quark phase transition.

In this Letter, we propose a scheme to determine the hadron–quark phase transition region via astronomical observations. The starting point of our scheme is constructing the speed of sound in the matter and the EoS with well established approaches for hadron matter and

quark matter separately. The construction takes the baryon chemical potentials which correspond to the beginning and the ending of the phase transition as parameters. With the mass, the radius and the tidal deformability of neutron stars being taken as calibrations to exclude the inappropriate parameters, we propose the possible baryon chemical potential range for the hadron-quark phase transition to happen in cold dense matter.

Construction of the Complete EoS: As known, the hadron matter and the quark matter are usually described via different approaches. For the hadron matter, we adopt the relativistic mean field theory with TW-99 parameterization [17, 18], and for the quark matter, we adopt the Dyson-Schwinger equation approach with parameter $\alpha = 2$ [18, 19]. By implementing the Gibbs construction scheme [7], we deduce the EoS $p(\varepsilon)$ for the hybrid star matter, and the speed of sound is simply $c_s^2 = (\partial p / \partial \varepsilon)$.

The calculated sound speed squared as a function of baryon chemical potential is shown in Fig. 1. At low baryon chemical potential, the matter is in hadron phase, then the speed of sound increases monotonically with the increasing of baryon chemical potential. At $\mu_0 = 1.23$ GeV, the quark matter begins to appear, and the speed of sound gets discontinuous. The sound speed involves another gap at $\mu_1 = 1.63$ GeV, where hadron matter disappears totally and the hadron-quark phase transition ends.

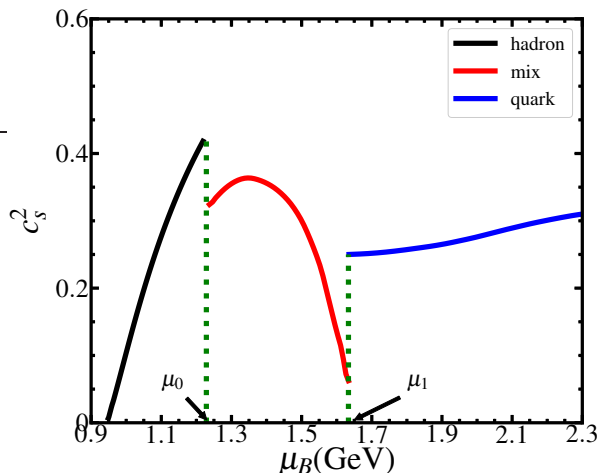


FIG. 1. (color online) Calculated sound speed squared as a function of baryon chemical potential. The hadron matter is described with the TW-99 model in the RMF theory and contains only protons and neutrons (and leptons). The quark matter is described with the DS equation of QCD with $\alpha = 2$. The mixed phase is described with the Gibbs construction.

However, since both the hadron model and the quark model are inaccurate at densities where the phase transition takes place, the calculated critical baryon chemical potential loses its accuracy. Also, in our previous work [18], we showed that if we take the Gibbs construc-

tion to build the complete EoS, the maximum mass of the hybrid star can not reach $2M_\odot$ even if we don't include hyperons. We have also shown that, if we include hyperons in the hadron model, the phase transition will not occur under Gibbs construction. Therefore, we need to find another scheme to construct the EoS.

In the spirit of 3-window construction, we can get the EoS of the matter in the middle density region by interpolating the results of the hadron model and the quark model. There have been methods to interpolate the $p_H(\mu_B)$ and the $p_Q(\mu_B)$ using a polynomial function [20], and to interpolate the $\varepsilon_H(\rho_B)$ and the $\varepsilon_Q(\rho_B)$ using hyperbolic weight function [21]. However, these interpolation scheme cannot take into consideration of the characteristics of the first order phase transition.

To avoid the problems encountered in the 3-window construction, we propose then to make use of the variation feature of the sound speed to construct the EoS now. In low chemical potential region, the speed of sound is calculated using the RMF model. In high chemical potential region, the speed of sound is calculated via the DS equation approach. Inspired by the result obtained via the Gibbs construction, the speed of sound in the middle region is constructed with a quadratic function:

$$c_M^2(\mu_B) = A\mu_B^2 + B\mu_B + C, \quad (1)$$

where A , B and C are parameters. The range of the phase transition region is noted as $\mu_0 \leq \mu_B \leq \mu_1$, where μ_0 and μ_1 correspond to the beginning and the ending of the phase transition.

After constructing the speed of sound as a function of baryon chemical potential with five parameters A , B , C , μ_0 and μ_1 , we can calculate the EoS of the matter by solving the equations

$$\frac{\partial \rho_B}{\partial \mu_B} = \frac{\rho_B}{\mu_B c_s^2(\mu_B)}, \quad \frac{\partial p}{\partial \mu_B} = \rho_B, \quad (2)$$

which are just simply the thermodynamic relations. The boundary condition is

$$\rho_B(\mu_0) = \rho_H(\mu_0), \quad p(\mu_0) = p_H(\mu_0), \quad (3)$$

where ρ_H and p_H is the baryon number density and the pressure calculated using the hadron model.

However, in high density region, although the sound speed is the same, the constructed EoS and the quark matter's EoS may have a constant difference. Therefore, we require:

$$p(\mu_1) = p_Q(\mu_1), \quad \rho_B(\mu_1) = \rho_Q(\mu_1), \quad (4)$$

where p_Q and ρ_Q is the pressure, the baryon number density of the quark matter, respectively. We take Eq.(4) to constrain the parameters. Then only three of the five parameters are independent.

In order to fix the interpolation of the sound speed squared, we need three of the five parameters: A , B ,

C , μ_0 and μ_1 , because of the quadratic relation. Equivalently, in this work, we take the sound speed squared $c_s^2(\mu_{\text{middle}})$ to be a free parameter, where $\mu_{\text{middle}} = (\mu_0 + \mu_1)/2$. The three independent parameters are then set as μ_0 , μ_1 and $c_s^2(\mu_{\text{middle}})$.

In our calculation, the ranges of these parameters are set as: $0.93 \leq \mu_0 \leq 1.5\text{GeV}$, $1.2\text{GeV} \leq \mu_1 \leq 2.0\text{GeV}$, $0 \leq c_{\text{middle}}^2 < 1.0$. We randomly choose these parameters from their corresponding ranges and construct the square of the sound speed, then deduce the EoS in each case. We do this for 200000 times, and get a large number of values of the sound speed squared and the EoS.

Since the constructed sound speed should be qualitatively the same as that calculated with the Gibbs construction, we also require that the sound speed in the mixed phase is smaller than that of pure hadron and quark matter at μ_0 , μ_1 , respectively (see Fig. 1).

Numerical Results and Discussions: After having the EoS of the dense matter, we can calculate the mass-radius relation of the compact star composed of the matter by solving the TOV equation (see, e.g., Ref. [7]). The tidal deformability Λ can also be calculated along the line of Refs. [22, 23].

Since neutron stars with masses about $2M_\odot$ has been observed [13, 14], we exclude the constructed EoSs which result in a maximum mass less than $2M_\odot$. The detection of gravitational wave GW170817 also sets the upper limit of the maximum mass of neutron stars, so we require that the maximum mass is less than $2.16M_\odot$ [24–26]. Based on the information provided by the gravitational wave detection for the tidal deformability Λ , we require $\Lambda_{1.4} < 800$ for a $1.4M_\odot$ neutron star according to Ref. [16], and $\Lambda_{1.4} > 120$ according to Ref. [27]. Since the neutron star radius also depends on the model, we take $9.9 < R < 13.6\text{km}$ for $1.4M_\odot$ neutron star according to Ref. [27] to constrain the EoS. Here the neutron star refers to the star whose composing matter involves the hadron-quark phase transition. The baryon chemical potential for the hadron-quark phase transition to occur can then be constrained by the astronomical observations.

In Fig. 2, we show the μ_0 dependence of the number of the EoSs satisfying several kinds of astronomical constraints. We show the number of the EoSs without any astronomical constraints with red bars, those satisfying the requirement $120 < \Lambda_{1.4} < 800$, $9.9 < R_{1.4} < 13.6\text{km}$ with blue bars, those with further constraint $M_{\text{max}} > 2M_\odot$ with yellow bars, and the ones with much further requirement $2M_\odot < M_{\text{max}} < 2.16M_\odot$ in green bars. Although the parameters are taken randomly in the corresponding ranges, the red bars which label the number of the EoSs without any astronomical constraint shown in Fig. 2 is not uniformly distributed. This is because when μ_0 is too large, there are possibilities for $\mu_0 > \mu_1$, or the construction cannot satisfy the boundary condition in Eq. (4). From Fig. 2, one can find easily that,

although the constraints on the tidal deformability and the radius reduce the number of the EoSs for different values of the μ_0 , they do not change the range of the μ_0 . Meanwhile the lower limit of the maximum mass reduces the upper limit of the μ_0 , but the upper limit of the maximum mass doesn't change the range of μ_0 . After taking into account all the astronomical constraints, the range of μ_0 is constrained to be $\mu_0 \leq 1.12\text{GeV}$, which corresponds to a baryon number density $n_0 \leq 3.16n_s$, where $n_s = 0.153\text{fm}^{-3}$ is the saturation density. However, the lower limit of μ_0 is only 0.94GeV , corresponding to nearly zero baryon number density which is consistent with the DS equation result given in Ref. [28].

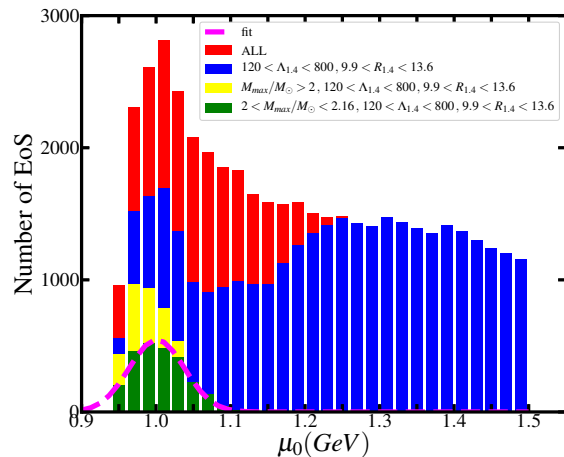


FIG. 2. (color online) Calculated μ_0 dependence of the number of constructed EoSs with several kinds of astronomical constraints. In the construction, the hadron matter is described with the TW-99 model with nucleons and hyperons, and the quark matter is described via the DS equation approach with $\alpha = 2$. Different colors correspond to different astronomical constraints. The pink dashed line is the fit of the green bars using Gaussian distribution.

Since our initial parameters are randomly distributed in their corresponding ranges, the number of the EoSs should be proportional to the probability distribution. Therefore, we make use of a Gaussian distribution function to fit the number distribution of the green bars in Fig. 2, and the fitted result is plotted in the figure with pink dashed line. The most probable value of the μ_0 is $\langle \mu_0 \rangle = 1.01\text{GeV}$, corresponding to a baryon number density $1.64n_s$ at which the nucleons in the matter begin to overlap with each other [29].

Similar analysis can also be carried out on the μ_1 , the baryon chemical potential corresponding to the ending of the hadron–quark phase transition. The obtained results of the μ_1 dependence of the number of the EoSs satisfying different astronomical constraints are displayed in Fig. 3.

After applying the astronomical constraints, the range of μ_1 is assigned as $1.42 \leq \mu_1 \leq 1.65\text{GeV}$, corresponding to a baryon number density range $6.13 \leq n_1/n_s \leq 11.14$.

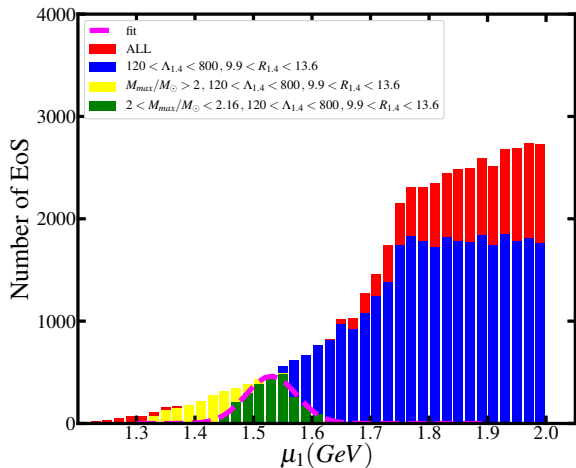


FIG. 3. The same as Fig. 2 but for the μ_1 dependence.

As the same as done in Fig. 2, we fit the green bars with Gaussian distribution function, and find that the most probable chemical potential is $\langle \mu_1 \rangle = 1.53$ GeV, which corresponds to $\langle n_1 \rangle = 8.22 n_s$.

We have shown above that astronomical observations can constrain the chemical potential of the phase transition. However, the ranges of the astronomical observables, e.g., the mass, the tidal deformability and the radius have not yet been fixed concretely in observations, and different studies give distinct results. Thereafter, we repeat the above described analyzing process with different astronomical constraints, and for each set of the constraints, we consider two different cases: hyperons appear or do not appear in the hadron matter. The main characteristics of the results in case of without and with hyperons are listed in Table I.

The first set of Table I gives the result with the astronomical constraints we have just used. The notation Nq, NYq refers to the case that the hadron matter sector does not include, or includes hyperons, respectively. Comparing the results with and without hyperons, one can observe that the upper limit of the μ_0 decreases after including hyperons. The second set lists the result when a larger upper limit of the maximum mass of a star is taken. It is evident that, the lower limit of the μ_1 reduces a lot, no matter whether hyperons are included. The third set shows the result under a larger lower limit of the tidal deformability. It manifests clearly that the upper limits of the μ_1 is reduced. Meanwhile the upper limit of the μ_0 is also reduced when hyperons are included. The fourth set shows the result under a smaller radius range. One can notice from the data that the upper limit of the μ_1 is reduced, but the change is smaller comparing to the second and the third set. This means that the constraints from the mass and the tidal deformability is more stringent.

The obtained result under the most strict astronomical constraints is given in the last set of Table I. It is appar-

ent that the ranges of the μ_0 and the μ_1 are narrowed down correspondingly. Furthermore, under these constraints, the most probable beginning and ending chemical potentials are $\langle \mu_0 \rangle = 1.08$ GeV, $\langle \mu_1 \rangle = 1.50$ GeV in the case without hyperons, and $\langle \mu_0 \rangle = 0.99$ GeV and $\langle \mu_1 \rangle = 1.49$ GeV when hyperons are included. It indicates that the chemical potential corresponding to the ending of hadron-quark phase transition is not influenced much by the inclusion of hyperons under such an astronomical circumstance, but the chemical potential corresponding to the beginning of the phase transition is obviously reduced by hyperons.

Summary: In this Letter, we propose a novel way to interpolate the hadron and the quark models to construct a complete EoS for the compact star matter involving hadron-quark phase transition. We take the speed of sound in the matter as the objective quantity to be interpolated, with which one can take into consideration the characteristics of the first-order phase transition, since the sound speed changes abruptly at both the beginning and the ending points of the phase transition. To describe the hadron matter we take the RMF model with the TW-99 parameters, and for the quark matter we implement the Dyson-Schwinger equation approach of QCD.

With the astronomical observation constraints such as the maximum mass of a neutron star, the radius and the tidal deformability of the star with 1.4 times the solar mass being taken as calibrations, the baryon chemical potentials which correspond to the beginning and the ending of the phase transition are constrained to a small range. Meanwhile the distribution of the phase transition chemical potentials can be fitted with the Gaussian distribution, and the most probable values of the phase transition chemical potential and baryon number density are found. The obtained results agree with the ones given via effective field theory of QCD very well.

We have also looked over the effect of the maximum mass, the radius, and the tidal deformability on the phase transition chemical potentials by varying the calibration ranges of the observables. It shows that a narrower range of the astronomical values indeed leads to a narrower range of the phase transition chemical potential. With the most strict observation constraints, the most probable values of the hadron-quark phase transition chemical potential and the baryon density are: $\langle \mu_0 \rangle = 0.99$ GeV and $\langle \mu_1 \rangle = 1.49$ GeV, i.e., $\langle n_0 \rangle = 1.39 n_s$ and $\langle n_1 \rangle = 7.43 n_s$.

Even though the phase transition chemical potentials have not yet been constrained to concrete values exactly now, we have shown that the presently proposed scheme to determine the baryon chemical potential region for the hadron-quark phase transition to occur is efficient and found the most probable values of the phase transition chemical potentials. With future detections, the maximum mass, the tidal deformability and the radius

TABLE I. Constrained quantities featuring the hadron-quark phase transition under different astronomical observations. The composition Nq, NYq refers to the case that the hadron matter sector does not include, or include hyperons, respectively. The baryon chemical potentials are in the unit of GeV, and the baryon number densities are in the unit of n_s .

Astronomical observations			composition	Constrained Range of the quantities									
$M_{\max}(M_{\odot})$	$\Lambda_{1.4}$	$R_{1.4}(\text{km})$		$\mu_{0\max}$	$n_{0\max}$	$\langle\mu_0\rangle$	$\langle n_0\rangle$	$\mu_{1\min}$	$\mu_{1\max}$	$n_{1\min}$	$n_{1\max}$	$\langle\mu_1\rangle$	$\langle n_1\rangle$
2-2.16	120-800	9.9-13.6	Nq	1.32	4.11	1.03	1.88	1.42	1.66	6.06	11.37	1.51	7.87
			NYq	1.12	3.16	1.01	1.64	1.42	1.65	6.13	11.14	1.53	8.22
2-2.35	120-800	9.9-13.6	Nq	1.32	4.11	1.00	1.57	1.31	1.66	4.57	11.36	1.50	7.64
			NYq	1.12	3.16	0.99	1.38	1.31	1.65	4.56	11.14	1.50	7.59
2-2.16	344 [30]-800	9.9-13.6	Nq	1.32	4.11	1.08	2.39	1.42	1.58	6.06	9.25	1.50	7.62
			NYq	1.05	2.31	0.99	1.35	1.42	1.59	6.13	9.52	1.49	7.39
2-2.16	120-800	10.62-12.83 [31]	Nq	1.32	4.11	1.04	1.99	1.42	1.61	6.06	10.13	1.51	7.84
			NYq	1.12	3.16	1.01	1.63	1.42	1.63	6.13	10.72	1.52	8.07
2-2.16	344-580 [32]	10.62-12.83	Nq	1.32	4.11	1.08	2.39	1.42	1.58	6.06	9.24	1.50	7.62
			NYq	1.05	2.31	0.99	1.39	1.44	1.59	6.40	9.52	1.49	7.43

of neutron stars can be measured with higher accuracy, the range of the phase transition chemical potentials can be determined with high precision.

The work was supported by the National Natural Science Foundation of China under Contracts No. 11435001, No. 11775041, and the National Key Basic Research Program of China under Contract No. 2015CB856900.

* baizhan@pku.edu.cn

† Corresponding author: yxliu@pku.edu.cn

- [1] H.T. Ding, F. Karsch, and S. Mukherjee, *Int. J. Mod. Phys. E* **24**, 1530007 (2015).
- [2] C. D. Roberts and S. Schmidt, *Prog. Part. Nucl. Phys.* **45**, S1 (2000); A. Bashir, L. Chang, I. C. Cloet, B. El-Bennich, Y. X. Liu, C. D. Roberts, and P. C. Tandy, *Commun. Theor. Phys.* **58**, 79 (2012).
- [3] S. X. Qin, L. Chang, H. Chen, Y. X. Liu, and C. D. Roberts, *Phys. Rev. Lett.* **106**, 172301 (2011); X.Y. Xin, S.X. Qin, and Y. X. Liu, *Phys. Rev. D* **90**, 076006 (2014); F. Gao, J. Chen, Y. X. Liu, S. X. Qin, C. D. Roberts, and S. M. Schmidt, *Phys. Rev. D* **93**, 094019 (2016); F. Gao and Y. X. Liu, *Phys. Rev. D* **94**, 076009 (2016).
- [4] C. S. Fischer, *Prog. Part. Nucl. Phys.* **105**, 1 (2019).
- [5] T. K. Herbst, J. M. Pawłowski, and B.-J. Schaefer, *Phys. Rev. D* **88**, 014007 (2013).
- [6] K. Fukushima and V. Skokov, *Prog. Part. Nucl. Phys.* **96**, 154 (2017).
- [7] N. K. Glendenning, *Compact Stars: Nuclear Physics, Particle Physics, and General Relativity* (Springer-Verlag, Berlin, 2000).
- [8] G. Baym, T. Hatsuda, T. Kojo, P.D. Powell, Y.F. Song, and T. Takatsuka, *Rep. Prog. Phys.* **81**, 056902 (2018).
- [9] Z.G. Xiao, B.A. Li, L.W. Chen, G.C. Yong, and M. Zhang, *Phys. Rev. Lett.* **102**, 062502 (2009).
- [10] M. Oertel, M. Hempel, T. Klähn, S. Typel, *Rev. Mod. Phys.* **89**, 015007 (2017).
- [11] J.M. Lattimer and M. Prakash, *Science* **304**, 536 (2004).
- [12] F. Weber, R. Negreiros, P. Rosenfield, and M. Stejner, *Prog. Part. Nucl. Phys.* **59**, 94 (2007).
- [13] P.B. Demorest, T. Pennucci, S.M. Ransom, M.S.E. Roberts, and J.W.T. Hessels, *Nature* **467**, 1081 (2010).
- [14] J. Antoniadis *et al.*, *Science* **340**, 1233232 (2013).
- [15] B. P. Abbott *et al.*, *Astrophys. J. Lett.* **848**, L13 (2017).
- [16] Abbott *et al.*, *Phys. Rev. Lett.* **119**, 161101 (2017).
- [17] S. Typel and H.H. Wolter, *Nucl. Phys. A* **656**, 331 (1999).
- [18] Z.Bai, H. Chen, and Y. X. Liu, *Phys. Rev. D* **97**, 023018 (2018).
- [19] H. Chen, M. Baldo, G. F. Burgio *et al.*, *Phys. Rev. D* **84**, 105023 (2011).
- [20] T. Kojo, P.D. Powell, Y. Song, and G. Baym, *Phys. Rev. D* **91**, 045003 (2015).
- [21] K. Masuda, T. Hatsuda, and T. Takatsuka, *Prog. Theor. Exp. Phys.* **7**, 073D01 (2013).
- [22] É. É. Flanagan and T. Hinderer, *Phys. Rev. D* **77**, 021502 (2008); T. Hinderer, *Astrophys. J.* **677**, 1216 (2008).
- [23] T. Zhao and J. M. Lattimer, *Phys. Rev. D* **98**, 063020 (2018).
- [24] B. Margalit and B. Metzger, *Astrophys. J.* **850**, L19 (2017).
- [25] L. Rezzolla, E. R. Most and L. R. Weih, *Astrophys. J.* **852**, L25 (2018).
- [26] M. Ruiz, S. L. Shapiro, and A. Tsokaros, *Phys. Rev. D* **97**, 021501 (2018).
- [27] E. Annala, T. Gorda, A. Kurkela, and A. Vuorinen, *Phys. Rev. Lett.* **120**, 172703 (2018).
- [28] F. Gao and Y.X. Liu, *Phys. Rev. D* **94**, 094030 (2016).
- [29] Y. X. Liu, D.F. Gao, and H. Guo, *Nucl. Phys. A* **695**, 353 (2001); L. Chang, Y. X. Liu, and H. Guo, *Nucl. Phys. A* **750**, 324 (2005).
- [30] T. Malik, N. Alam, M. Fortin, C. Providência, B. K. Agrawal, T. K. Jha, Bharat Kumar, and S. K. Patra, *Phys. Rev. C* **98**, 035804 (2018).
- [31] J. M. Lattimer and A. W. Steiner, *Eur. Phys. J. A* **50**, 40 (2014).
- [32] B. P. Abbott *et al.*, *Phys. Rev. Lett.* **121**, 161101 (2018).